

# Adaptive reference voltage-based MPPT technique for PV applications

ISSN 1752-1416

Received on 15th September 2016

Revised 18th December 2016

Accepted on 12th January 2017

E-First on 21st March 2017

doi: 10.1049/iet-rpg.2016.0749

www.ietdl.org

Mohamed Lasheen<sup>1</sup> , Ali Kamel Abdel Rahman<sup>1</sup>, Mazen Abdel-Salam<sup>2</sup>, Shinichi Ookawara<sup>3</sup>

<sup>1</sup>Department of Energy Recourses Engineering, Egypt-Japan University of Science and Technology (E-JUST), PO Box 179, New Borg El-Arab City 21934, Alexandria, Egypt

<sup>2</sup>Electrical Engineering Department, Assiut University, Assiut, Egypt

<sup>3</sup>Chemical Science and Engineering Department, Tokyo Institute of Technology, Tokyo, Japan

✉ E-mail: mohamed.lasheen@ejust.edu.eg

**Abstract:** The constant voltage (CV) for maximum power point tracking (MPPT) technique is considered one of the most commonly used techniques in the photovoltaic (PV) applications. This study is aimed at proposing an adaptive reference voltage-based MPPT technique (ARV) to improve the performance of the CV technique by making it adaptable to weather conditions. The RV for MPPT is adapted according to the measured radiation and temperature levels. The operating range of the radiation at a given temperature is divided into number of divisions and the corresponding RV is recorded off-line in a truth table. The difference between the reference and measured PV voltages is compensated using proportional–integral controller to generate suitable duty ratio to the boost converter. Performance assessment of the CV technique after being improved covers time response, MPPT efficiency, oscillation and stability. The results present performance improvement by fast time response to reach steady-state value, more stable operation with no oscillation and high MPPT efficiency as compared with the CV technique without the proposed improvement.

## 1 Introduction

Recently, the world energy demand is increasing due to the increase in technology development, standard of living and world population. In addition, the energy generation from clean, efficient and environmentally friendly sources has become one of the major challenges for engineers and scientists, due to the limited reservoirs of fossil fuels and emission of greenhouse gases. Renewable energy is expected to have large potential as an alternative energy source without constraint on energy supply or greenhouse gas emissions [1–3].

At present, photovoltaic (PV) generation is assuming increased importance as a renewable energy application because of distinctive advantages such as simplicity of allocation with no fuel cost, low maintenance, lack of noise due to the absence of moving parts and declining prices and increasing efficiency of solar cells [4–8].

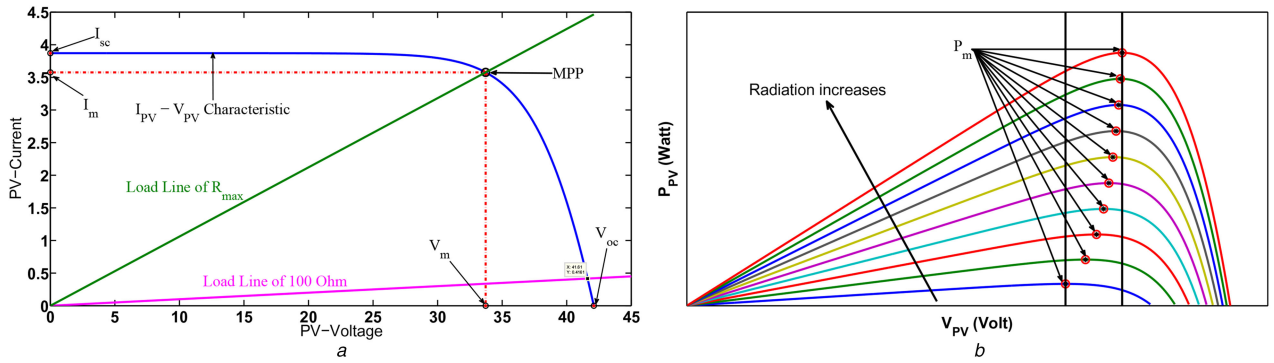
### 1.1 Problem formulation

Fig. 1a shows that the power generated by PV module is dependent on a number of atmospheric conditions (solar radiation and temperature) and the load resistance  $R$ ; there is a specific load  $R_{\max}$ , which can capture maximum available power  $P_m$  at given atmospheric conditions, Fig. 1a. To follow weather variations to seek maximum available power, an interface DC–DC converter has to be used and controlled by suitable maximum power point tracking (MPPT) technique in order to change the PV operating point to be at the MPP and to make the PV module seeing the connected load as its  $R_{\max}$  [2, 9, 10]. Among all the MPPT techniques, the constant voltage (CV) technique is one of the most commonly used techniques in PV applications. Therefore, the purpose of this work is to improve the performance of the CV technique for making it adaptable to weather conditions in tracking MPP. The five-parameters precise model of the PV module and the boost converter model including all the uncertainties (parasitic resistances,  $r_i$  for inductor,  $r_c$  for capacitor and  $r_d$  for diode) are considered for the investigated PV system seeking more precision of the proposed MPPT technique. Thus, this paper is organised as

follows: review on CV technique-based MPPT is presented in Section 2. Followed by the proposed adaptive reference voltage (ARV)-based MPPT technique in Section 3. Next, system configuration is described in Section 4 to assess the performance of the CV technique after being improved. After that, the results and discussion are presented in Section 5. Finally, the conclusions of the paper are reported in Section 6.

## 2 Review on CV technique-based MPPT

Over 60 decades until nowadays, the MPPT techniques were investigated through more than about 100 scientific research documents [9]. The differences among them are in many aspects, e.g. accuracy, simplicity, velocity, hardware implementation, sensing elements, range of effectiveness, need for parameterisation and financial view. The proposed techniques can be broadly classified as short-current pulse [11–13], incremental conductance [14–16], hill climb [17–19] and CV [20–28]. There are another MPPT techniques, which depend on estimation technique [29, 30] or on an artificial intelligence algorithms [4, 31]. The performance of different MPPT techniques was compared before [2, 9, 10, 26, 32]. They claimed that most of the presented techniques in the literature suffer from the drawback of poor stability with a possibility of producing oscillations in output power due to the highly non-linear characteristics of the PV module. In addition to that, the conventional techniques such as hill climb [17–19] cannot quickly acquire the MPPs for the power generated by PV modules. This concludes that the CV technique is the simplest MPPT technique compared with those presented before [20–28], as it uses one sensor with no need for complicated computation. The CV technique uses proportional–integral (PI) controller, Fig. 2a, which makes its performance fast and robust. Moreover, the PI controller is used to determine the duty ratio  $d$  of the DC–DC converter by regulating the error signal between module output voltage and aRV  $V_{\text{ref}}$ . According to [20, 21, 24, 26, 28], the CV technique utilises empirical results, indicating that the voltage at the MPP  $V_m$  is about 70–80% of the solar cell open-circuit voltage. This provides a reference to which the output voltage can be forced to track. Measurement of the open-circuit voltage calls for a momentary



**Fig. 1** PV module characteristics

(a)  $I_{PV}$  –  $V_{PV}$  characteristic, (b) Typical  $P_{PV}$  –  $V_{PV}$  curves at varying radiation levels

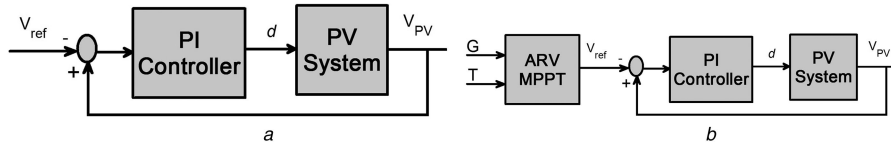


**Fig. 2** Schematic block diagram of

(a) CV MPPT technique, (b) ARV MPPT technique

interruption of PV power. In an attempt [22, 23], the solar module source was configured to sample its open-circuit voltage without breaking the entire source from the load. Some investigators [25, 27] used CV technique, where  $V_{ref}$  is assumed a fixed value for the MPP voltage equal to the value measured at standard test conditions (STCs) provided by the manufacturer of the PV module. This assumes that weather variations are insignificant to affect the module output voltage.

The above survey concludes the main problems with conventional CV-based MPPT technique, which are either it requires a momentary interruption of PV power, or it assumes that radiation and temperature variations are insignificant to affect the generated power from the PV module. These problems result wasting significant part of the available power.

### 3 Proposed ARV-based MPPT technique

This section proposes an ARV-based MPPT technique in order to take the weather variations into consideration without any interruption for the PV generation system.

For the same operating temperature, Fig. 1b represents typical  $P_{PV}$  –  $V_{PV}$  curves for a PV module at ascending radiation levels with constant increment. It depicts that the range of  $V_m$  over this operating radiation range is small as shown between two black vertical straight lines. The span between two successive radiation levels is so small to the extent that  $V_m$  for any radiation level within the span could serve as the RV  $V_{ref}$  for the PI controller. The maximum voltage  $V_m$  for each span is recorded off-line in a truth table and is used as the RV to adjust the duty ratio of an MPPT converter, Fig. 2b. The proposed ARV technique does not necessitate momentary interruption of PV module and takes into consideration the weather conditions by measuring the temperature and radiation levels using two extra sensors when compared with the classical CV technique, which uses only one sensor for voltage measurement. This represents an improvement of the CV technique and makes it as ARV-based MPPT technique.

The advantages of the proposed ARV technique are clearly presented in Section 5, especially when compared with the well-known perturb and observe (P&O) technique [9], as shown in Fig. 8b. Moreover, this ARV technique calls for simple computations when compared with complicated computations as proposed by others [3] for MPPT. It is quite clear that the smaller the span the higher is the MPPT efficiency being defined in detail in Section 5. This calls for increasing the size of the truth table. However, this does not represent a disadvantage in the light of huge memories, which are currently available for data storage of

the controller. Even though, it uses two extra sensors more than the CV technique and one extra sensor more than the P&O technique, which uses two sensors. However, this is compensated by increasing the MPPT efficiency and the PV system stability as presented in Section 5.

The gains of this PI controller ( $K_p$  and  $K_i$ ) are determined by trial and error approach that results ( $K_p = 8.5$  and  $K_i = 85$ ). For trial and error approach, there are some rule of thumb for the effect of  $K_p$  and  $K_i$  on the system performance [33].  $K_p$  decreases rise time, increases overshoot and reduces steady-state error (SSE); while  $K_i$  increases rise time, decreases overshoot, increases settling time and eliminates SSE. Some general tips to follow are: (i) obtain an open-loop response and determine what needs to be improved. (ii) Add a P control to improve the rise time. (iii) Add an I control to eliminate the SSE. (iv) Adjust each of  $K_p$  and  $K_i$  until obtaining a desired overall response. The procedure for selecting  $K_p$  and  $K_i$  is described in Appendix 1.

### 4 System configuration

The proposed system comprises a PV module feeding a resistive load through pulse-width modulated boost converter.

#### 4.1 PV module

PV models can be categorised into two main types: double- and single-diode models [34], which are illustrated in Fig. 3. The double-diode model is characterised by its high accuracy [35]; however, it suffers from low computational speed as it is relatively complex [34]. Thus, the single-diode model is the most commonly used in power electronics simulation studies, because it offers a reasonable trade-off between accuracy and simplicity [36, 37]. In addition, its parameterisation depends only on provided information by data-sheet [30, 34, 37, 38]. The single-diode model shown in Fig. 3 consists of a current source, a diode and series and parallel resistances. The characteristics of PV module can be gotten from the second Kirchhoff law as [39]

$$I = I_{ph} - I_o \left\{ \exp \left( \frac{V + I \times R_s}{n_s \times V_t} \right) - 1 \right\} - \frac{V + I \times R_s}{R_{sh}} \quad (1)$$

where  $V$  and  $I$  are the voltage and current of the PV module, respectively; the five parameters (from which the five-parameters model obtains its name) are  $I_{ph}$ ,  $I_o$ ,  $V_t$ ,  $R_s$  and  $R_{sh}$ ;  $I_{ph}$  and  $I_o$  are the photo-generated current and the dark saturation current,

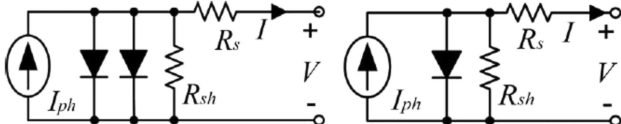


**Fig. 3** Equivalent circuits of double- and single-diode models

respectively;  $V_t$  is the junction thermal voltage;  $R_s$  and  $R_{sh}$  are the series and shunt resistances, respectively; and  $n_s$  is the number of series connected cells in the module. The junction thermal voltage of the diode is related to the junction temperature as:  $V_t = (k \times T \times A/q)$  where  $k$  is Boltzmann's constant,  $T$  is the junction temperature,  $A$  is the diode quality factor and  $q$  is the electron charge. The model represented by (1) has five unknown parameters:  $I_{ph}$ ,  $I_o$ ,  $V_t$ ,  $R_s$  and  $R_{sh}$ . The objective is to estimate these parameters under STC, and also under varying environmental conditions from data-sheet information provided by the manufacturer of this module. The data-sheet provides other four parameters at STC including short-circuit current  $I_{sc}$ , open-circuit voltage  $V_{oc}$ , operating voltage and current at MPP ( $V_m$ ,  $I_m$ ), Fig. 1a, and the number of cells  $n_s$  in the module connected in series. Sometimes,  $n_s$  is not given in the data-sheet. An approximate estimate of  $n_s$  was given as equal to:  $n_s \approx (V_{oc}/0.6)$ . This is because the  $V_{oc} \approx 0.6$  V for a single solar cell [40].

Substitution of the data-sheet points  $(0, I_{sc})$ ,  $(V_{oc}, 0)$  and  $(V_m, I_m)$  in (1) formulates three equations in the five unknown module parameters. The fourth equation is obtained at the MPP where  $dP/dV$  is equal to zero, where the output power  $P$  is obtained by multiplying (1) by the terminal voltage  $V$ . The fifth equation is concerned with the determination of the shunt resistance  $R_{sh}$ .  $R_{sh}$  was approximated as equal to inverse of the slope  $dI/dV$  at  $(0, I_{sc})$ . Simultaneous solution of the five formulated equations using Gauss-Seidel method [41] determines the five unknown parameters of the PV module at STC. The influence of temperature ( $T$ ) and radiation ( $G$ ) on the parameters is expressed in Appendix 2 [30, 38].

#### 4.2 Boost DC-DC converter

If the load directly coupled to the PV module, then it may capture the available maximum power or not depending on its resistance. Hence, this is compensated by an interface electronic device (DC-DC converter) that is used to operate as variable equivalent load as seen by the PV generation. The converter's duty ratio is used to adjust the equivalent load resistance as seen by the source, to transfer  $P_m$  from PV module to load demand. The three basic real topologies of DC-DC converter are buck, boost and buck-boost. Boost is used in this paper, as it is commonly used to boost the output PV voltage to be suitable with grid tie which is the most

application of PV generator [42, 43]. Fig. 4a shows a typical schematic block diagram to extract  $P_m$  from PV module using boost converter. The boost mathematical model is carried out by solving its governing (2) and (3) that are based on the state-space average method [44], which was successfully applied to pulse-width modulated power converters [45]. This method models switched converters as time independent systems, defined by a set of differential equations. Therefore, it can be a convenient approach for designing controllers to be applied to switched converters. As the boost converter contains two electrical storage elements (inductor  $L$  and capacitor  $C$ ), Fig. 4b. Therefore, two governing equations expressing the inductor current  $i_l$  and capacitor voltage  $v_c$  are written as [44]: (see (2))

$$\frac{dv_c}{dt} = \frac{1}{(R + r_c) \times C} \times [-v_c + R \times (1 - d) \times i_l] \quad (3)$$

where  $v_m$  and  $v_d$  are switch and diode forward voltages.  $V_i$  is the adjustable input voltage to the converter. The output voltage of the boost converter is expressed as [44]

$$V_o = \frac{R}{(R + r_c)} \times v_c + \frac{R \times r_c}{(R + r_c)} \times (1 - d) \times i_l \quad (4)$$

The inputs of boost mathematical model are  $V_i$  as obtained from PV mathematical model and  $d$  (duty ratio) as obtained from PI controller, while the outputs are inductor current and capacitor voltage.

**4.2.1 Boost converter design:** The designing of boost parameters ( $L$ ,  $C$  and diode) depends mainly on the available  $P_m$  from PV module and the connected load. The crucial quantities in the design of a boost circuit are inductor current ripple ( $\Delta I_l$ ) and output voltage ripple ( $\Delta V_o$ ).

For inductor selection [46]

$$L = \frac{V_i \times (V_o - V_i)}{\Delta I_l \times f_s \times V_o} \quad (5)$$

where  $V_i$  and  $V_o$  are the typical input voltage and desired output voltage, respectively.  $f_s$  is the minimum switching frequency of the converter.  $\Delta I_l$  is normally 20–40% of the output current. It is expressed as [46]

$$\Delta I_l = (0.2 \text{ to } 0.4) \times I_{o-\max} \times \frac{V_o}{V_i} \quad (6)$$

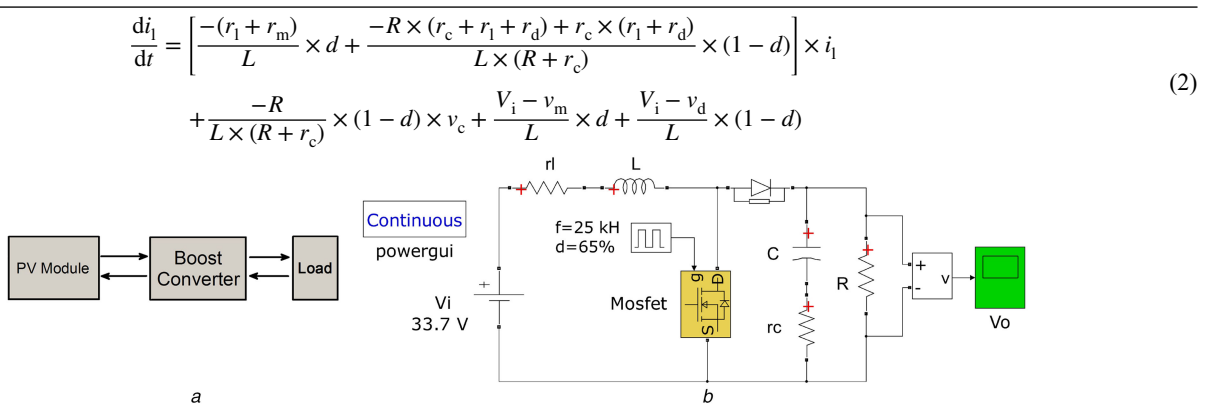


**Fig. 4** Details of MPPT system

(a) Block diagram, (b) MATLAB/Simulink model of boost converter

where  $I_{o-\max}$  is the maximum output current necessary for the load. However, this study estimated  $\Delta I_f = 20\%$  to ensure continuous operation mode and to guarantee the lowest output voltage ripple [46, 47].

For diode selection, the average forward current rating  $I_f$  needed is equal to  $I_{o-\max}$ .

For capacitor selection [46]

$$C_{o-\min} = \frac{I_{o-\max} \times d}{f_s \times \Delta V_o} \quad (7)$$

where  $C_{o-\min}$  and  $\Delta V_o$  are the minimum output capacitance and the desired output voltage ripple, respectively. The latter is selected in this study equal to 10 mV where the maximum allowed  $\Delta V_o$  is equal to 75 mV [48].

## 5 Results and discussion

To verify the performance of the proposed system as shown in Fig. 4a, it is simulated numerically by MATLAB (R2013b, 64 bit version) software using resistive load ( $R = 50 \Omega$ ). The case study is BP-MSX120 PV module, its specifications are tabulated in Table 1(a), where  $\kappa_i$  is the temperature coefficient of  $I_{sc}$  and  $\kappa_v$  is the temperature coefficient of  $V_{oc}$ , and the parameters of boost converter are grouped in Table 1(b).

### 5.1 PV characteristics

The proposed PV mathematical model is compared by power system simulator (PSIM)-based PV model, and the empirical curves associated with BP-MSX120 data-sheet through  $I-V$  characteristic at STC. The maximum deviation does not exceed  $\pm 0.5\%$ . The electrical characteristics of the PV module are demonstrated by  $I-V$  and  $P-V$  curves in Figs. 5a–c. The radiation and temperature influence the  $I-V$  characteristics as shown in Figs. 5a and b, respectively. Fig. 5a shows that both the short-circuit current and the open-circuit voltage increase with the increase of the radiation level. The short-circuit current increases

**Table 1** Key specifications

Parameter	Value
<b>(a) BP-MSX120 module</b>	
$P_m$	120 W
$V_m$	33.7 V
$I_m$	3.56 A
$I_{sc}$	3.87 A
$V_{oc}$	42.1 V
$\kappa_i$ and $\kappa_v$	0.065 and -0.16
$n_s$	72
$I_{ph-ref}$ and $I_{o-ref}$	3.871 and $4.47 \times 10^{-7}$ A
$R_s$ and $R_{sh}$	0.4471 and 1750 $\Omega$
$V_t$	0.0366 V
<b>(b) Boost converter</b>	
$V_i$	adjustable
$d$	controllable
$L$	0.05 H
$r_1$	0.2 $\Omega$
$C$	33 $\mu$ F
$r_c$	0.1 $\Omega$
$v_m$	0.07 V
$r_m$	0.01 $\Omega$
$v_d$	0.71 V
$r_d$	0.01 $\Omega$

linearly with the radiation level. However, the open-circuit voltage increases logarithmically with the radiation level. Fig. 5b shows that the open-circuit voltage decreases and the short-circuit current increases marginally with the increase of the operating temperature. Fig. 5c points out that the maximum output power increases with the increase of the radiation level. Figs. 5a–c show good agreement of the present PV module and that of PSIM.

### 5.2 Boost converter simulation

The proposed boost mathematical model is checked using MATLAB/Simulink, Fig. 4b. The solver of this model was ode45 (Dormand–Prince) with variable-step.

Fig. 5d shows the temporal variation of the converter output voltage as obtained by the proposed mathematical model. The agreement of the present computed temporal variation with that obtained using Simulink is very satisfactory, Fig. 5d.

Fig. 6a shows a surface [three-dimensional (3D) plot] giving PV MP  $P_m$  as influenced by radiation and temperature. This surface indicates that the available  $P_m$  from PV module increases with increase in radiation level and moderate temperature. Obviously, the radiation effect on PV power is dominant with respect to temperature. Therefore, the coming results are limited to the radiation effect only.

This paper divides radiation levels into 19 divisions 50, 100, ... up to 1000 W/m<sup>2</sup>. The voltage  $V_m$  corresponding to the MP is calculated off-line for each division. A sample of the values of  $V_m$  at standard temperature  $T(= 25^\circ\text{C})$  is recorded in Table 2.

The steady-state and transient performance of the proposed ARV and CV techniques along with its computed efficiency are investigated for the radiation profile as shown in Fig. 6b. It is worthy of mention that  $V_{ref}$  for the CV technique is selected as  $V_m$  from the data-sheet of the PV module that provided by the manufacturer [25]. Figs. 6c–7 show the increase of the output power  $P_{PV}$  and the decrease of the time  $t_{ss}$  to reach the steady-state value as predicted by the proposed ARV technique when compared with those obtained by the CV technique. The increase of  $P_{PV}$  and the decrease of  $t_{ss}$  are reported in Tables 3 and 4, respectively. The increase of  $P_{PV}$  reached 1.63% for the ARV technique with respect to the CV technique. The time  $t_{ss}$  assumed 150 ms for the ARV technique against 400 ms recorded by the CV technique for radiation of 400 W/m<sup>2</sup>. For radiation levels 700 and 800 W/m<sup>2</sup>,  $t_{ss}$  reached 3 ms for the ARV technique against 200 ms for the CV technique.

The MPPT efficiency  $\eta_{MPPT}$  was expressed before as [26, 49]

$$\eta_{MPPT} = \frac{\int P_{PV}(\text{MPPT technique}) dt}{\int P_{PV_{\max}}(\text{data - sheet}) dt} \quad (8)$$

The numerator of (8) is the computed output power based on the CV or the ARV technique. The denominator is the maximum output power computed using the module data-sheet after being corrected according the solar radiation and temperature.

Fig. 8a shows a histogram giving the increase of  $\eta_{MPPT}$  for the ARV technique when compared with that obtained by the CV technique at different radiation levels. This increase of MPPT efficiency is significant at low radiation levels and decreases gradually with the increase of the radiation level as shown in Fig. 8a. It is quite clear that  $P_{PV}$  and  $t_{ss}$  have the same values for both the CV and the ARV techniques at 1000 W/m<sup>2</sup>, Tables 3 and 4. This is simply attributed to the same  $V_{ref}$  for both techniques. The MPPT efficiency value obtained by the ARV technique can be increased if the number of the radiation divisions for the truth table increases higher than 19 depending on the available controller memory. For more improvement of tracking efficiency, more complex MPPT techniques would be required.

Sometimes the daily solar radiation assumes abrupt variations. This is why the performance of the proposed ARV technique under some abrupt radiation variations is investigated and compared with

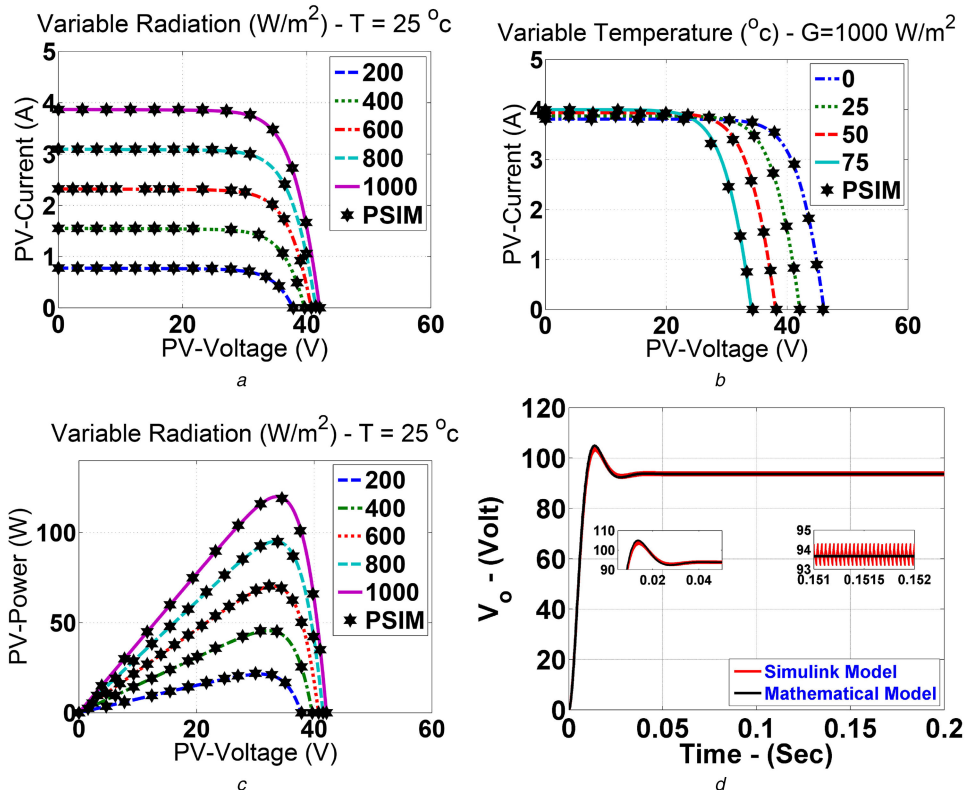


**Fig. 5** PV module and boost converter characteristics

(a) IPV – VPV curves as influenced by radiation, (b) IPV – VPV curves as influenced by temperature, (c) PPV – VPV curves as influenced by radiation, (d) Temporal variation of the boost output voltage

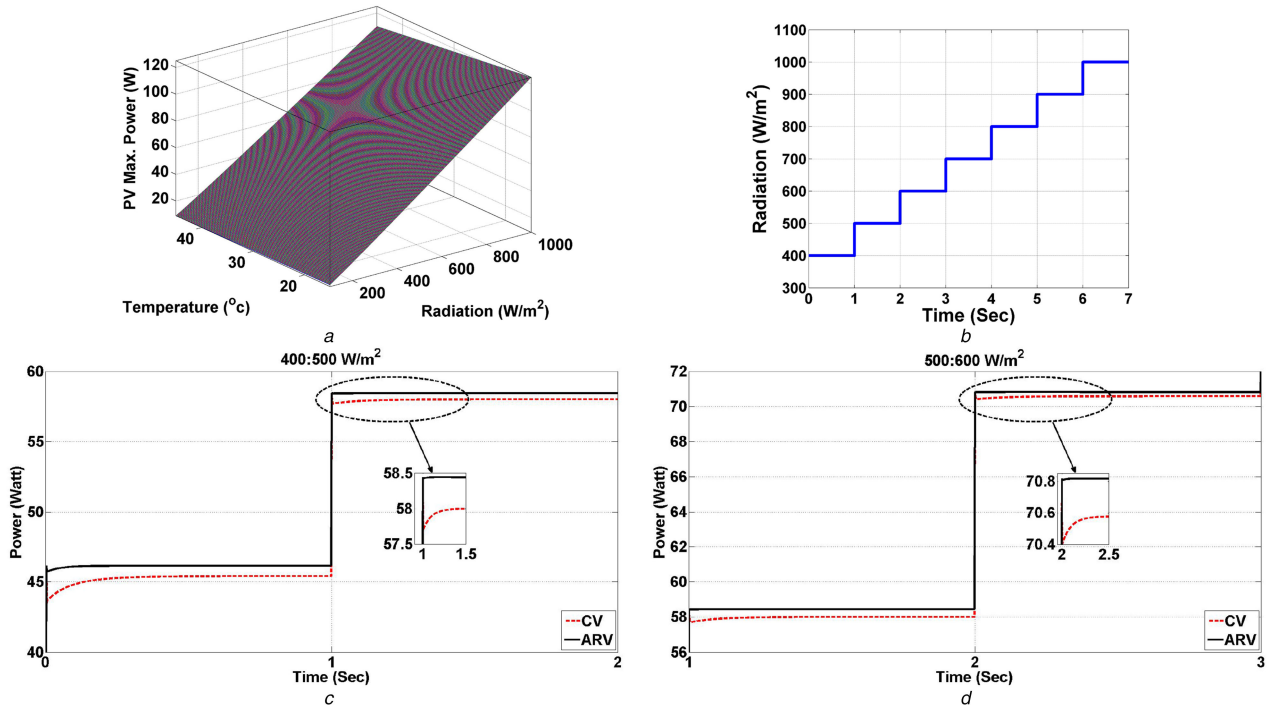


**Fig. 6** PV module output power

(a) Surface (3D plot) between two inputs ( $T$  and  $G$ ) and one output  $P_{\text{m}}$  (b) Radiation profile, (c) Effect of  $400 - 500 \text{ W/m}^2$  step change of radiation, (d) Effect of  $500 - 600 \text{ W/m}^2$  step change of radiation

the well-known P&O technique [9], as shown in Fig. 8b. This figure shows that the temporal variation of  $P_{\text{PV}}$  follows that of the radiation level. The tracking of the proposed technique is not affected greatly by radiation transients due to the fast response of the PI controller compared with variation of the radiation. This figure shows that the proposed ARV technique is faster when compared with the P&O technique in capturing the MPP. The

proposed technique is free from any oscillations as associated with the use of the P&O technique. Moreover, the P&O technique tracks the MPP only at distinct instants when the PV module is exposed to a radiation profile with fast rate of change. On the contrary, the proposed technique captures the MPP irrespective of the rate of change of the radiation profile. To validate the robustness of the proposed technique, a comparison is made in Fig. 8c between the

**Table 2**  $V_m$  for  $T = 25^\circ\text{C}$  and  $G = 400:50:1000 \text{ W/m}^2$ 

Radiation, $\text{W/m}^2$	$V_m, \text{V}$
400	32.2803
450	32.4999
500	32.689
550	32.8545
600	32.9987
650	33.1249
700	33.2386
750	33.3393
800	33.4272
850	33.507
900	33.5785
950	33.6424
1000	33.7

**Table 3**  $P_{PV}$  for CV and ARV at different radiations

Radiation, $\text{W/m}^2$	CV, W	ARV, W	% difference
400	45.4	46.14	1.63%
500	58	58.44	0.76%
600	70.57	70.82	0.354%
700	83.12	83.24	0.144%
800	95.63	95.68	0.052%
900	108.11	108.12	0.01%
1000	120.55	120.55	0.00

proposed ARV technique and that proposed before [3]. Fig. 8c shows variation around the MPP with less tracking accuracy [3] while the proposed ARV technique has no oscillations and better tracking accuracy.

## 6 Conclusion

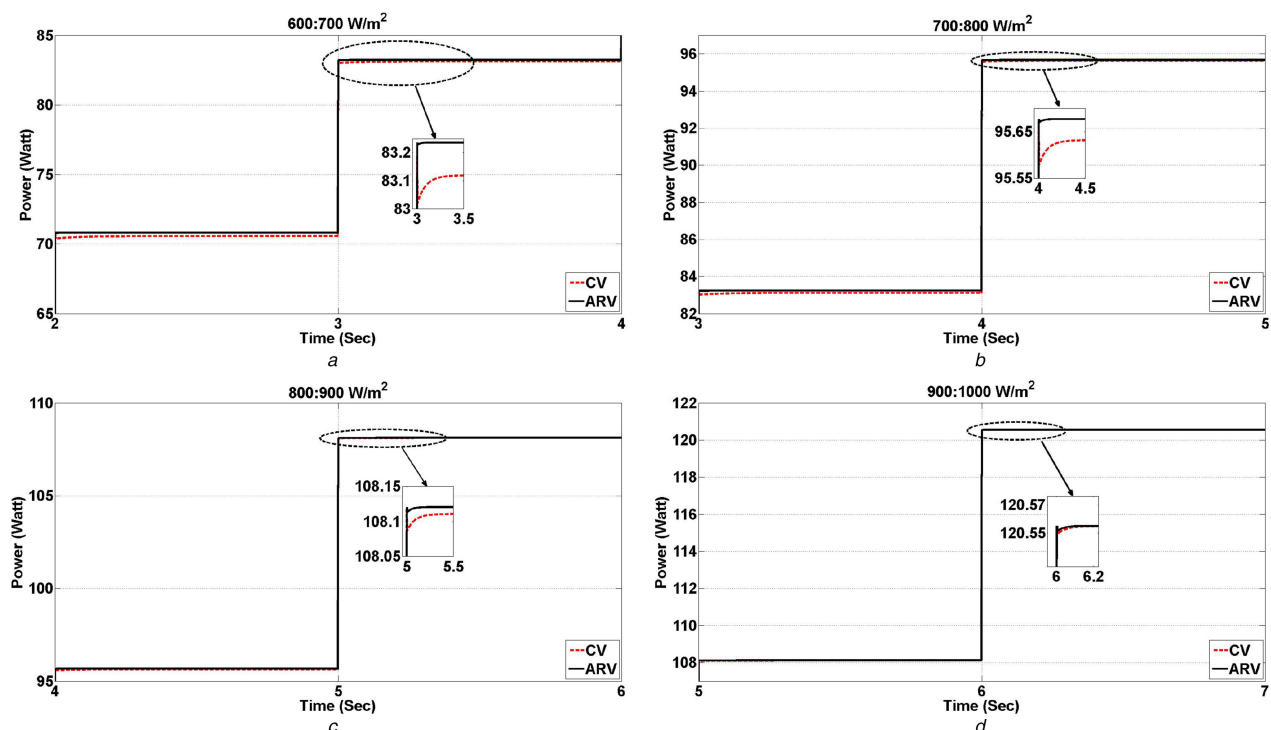
- An improvement of the CV technique is proposed to make it adaptable to weather changes including radiation and

temperature. This is why the RV for MPPT technique is made adaptable to weather changes.

- The proposed ARV technique showed an increase of the output power  $P_{PV}$  and a decrease of the time  $t_{ss}$  to reach the steady-state value when compared with those obtained by the CV technique.
- The proposed ARV technique showed an increase of MPPT efficiency  $\eta_{MPPT}$  when compared with that obtained by the CV technique at different radiation levels. This increase of MPPT efficiency is significant at low radiation levels and decreases gradually with the increase of the radiation level.
- The temporal variation of the output power  $P_{PV}$  as predicted by the proposed ARV technique followed that of the radiation level even with some abrupt variations of the radiation.
- The proposed ARV technique has no oscillations and better tracking accuracy when compared with observed variation around the MPP with less tracking accuracy [3].
- The proposed ARV technique is characterised by simple computations when compared with complicated computations proposed by others [3] for MPPT.
- The proposed technique captured the MPP even during fast rate of change of radiation without any oscillations when compared with the P&O technique.

## 7 Acknowledgments

The authors acknowledge the reviewers for their helpful comments, which enhanced the clarity of this paper. The first two authors acknowledge the Mission Department of the Ministry of Higher Education of Egypt for providing a scholarship to conduct this study as well as the Egypt – Japan University of Science and Technology (E-JUST) for offering the facility, tools and equipment needed to conduct this research work.

**Fig. 7** Temporal change of PV module output power as influenced by step change of radiation

(a)  $600 - 700 \text{ W/m}^2$ , (b)  $700 - 800 \text{ W/m}^2$ , (c)  $800 - 900 \text{ W/m}^2$ , (d)  $900 - 1000 \text{ W/m}^2$

**Table 4** Time to reach steady-state value for CV and ARV at different radiations

Radiation, W/m <sup>2</sup>	CV, ms	ARV, ms
400	400	150
500	200	4
600	200	4
700	200	3
800	200	3
900	150	3
1000	3	3

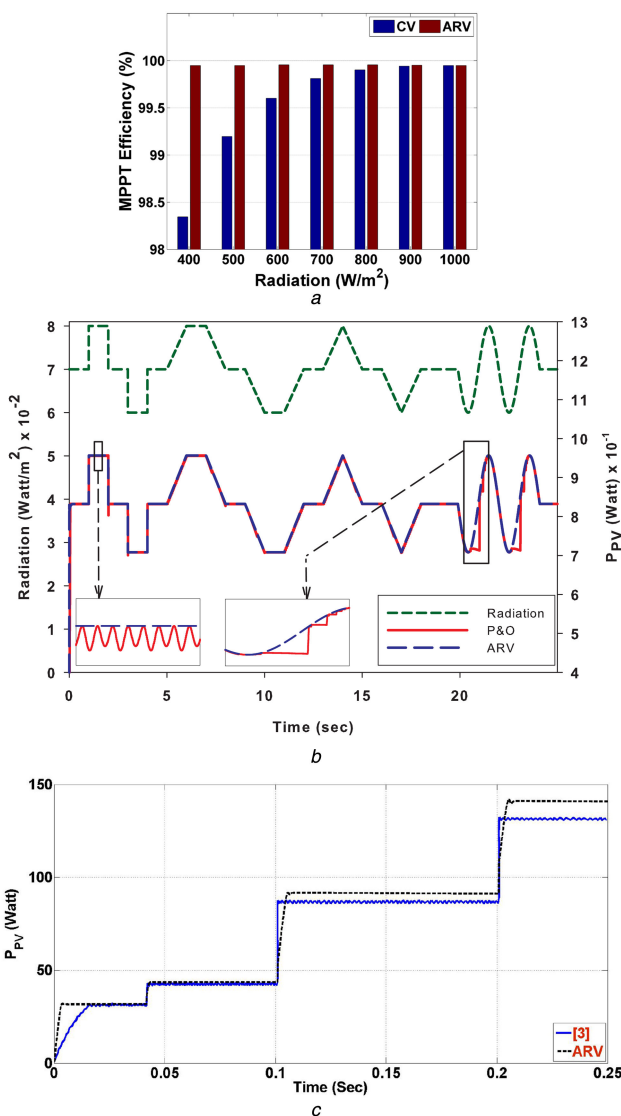


**Fig. 8** MPPT efficiency and PV module output power

(a) MPPT efficiency versus radiation, (b) Comparison between ARV technique and P&O technique at varying radiation profile, (c) Comparison between ARV MPPT technique and [3]

## 8 References

- [1] Solanki, C.S.: 'Solar photovoltaics: fundamentals, technologies and applications' (Delhi, PHI Learning Pvt. Ltd., 2015, 3rd edn.)
- [2] Faranda, R., Leva, S.: 'Energy comparison of MPPT techniques for PV systems', *WSEAS Trans. Power Syst.*, 2008, **3**, (6), pp. 446–455
- [3] Zainuri, M.A.A.M., Radzi, M.A.M., Soh, A.C., et al.: 'Development of adaptive perturb and observe-fuzzy control maximum power point tracking for photovoltaic boost dc–dc converter', *IET Renew. Power Gener.*, 2014, **8**, (2), pp. 183–194
- [4] Sefa, I., Altin, N., Ozdemir, S., et al.: 'Fuzzy PI controlled inverter for grid interactive renewable energy systems', *IET Renew. Power Gener.*, 2015, **9**, (7), pp. 729–738
- [5] Ahmad, Z., Singh, S.: 'Modeling and control of grid connected photovoltaic system – a review', *Int. J. Emerging Technol. Adv. Eng.*, 2013, **3**, (3), pp. 40–49
- [6] Hedayatizadeh, M., Ajabshirchi, Y., Sarhaddi, F., et al.: 'Thermal and electrical assessment of an integrated solar photovoltaic thermal (pv/t) water collector equipped with a compound parabolic concentrator (CPC)', *Int. J. Green Energy*, 2013, **10**, (5), pp. 494–522
- [7] Safari, A., Mekhilef, S.: 'Simulation and hardware implementation of incremental conductance MPPT with direct control method using cuk converter', *IEEE Trans. Ind. Electron.*, 2011, **58**, (4), pp. 1154–1161
- [8] Roger, M., Ventre, J.: 'Photovoltaic systems engineering' (The CRC Press, Boca Raton FL, USA, 2000, 3rd edn.)
- [9] Esram, T., Chapman, P.L.: 'Comparison of photovoltaic array maximum power point tracking techniques', *IEEE Trans. Energy Convers. EC*, 2007, **22**, (2), pp. 439–449
- [10] Dolara, A., Faranda, R., Leva, S.: 'Energy comparison of seven MPPT techniques for PV systems', *J. Electromagn. Anal. Appl.*, 2009, **1**, (3), pp. 152–162
- [11] Yuvarajan, S., Xu, S.: 'Photo-voltaic power converter with a simple maximum-power-point tracker'. Proc. Int. Symp. Circuits and Systems, 2003, vol. **3**, p. III-399
- [12] Noguchi, T., Togashi, S., Nakamoto, R.: 'Short-current pulse-based maximum-power-point tracking method for multiple photovoltaic-and-converter module system', *IEEE Trans. Ind. Electron.*, 2002, **49**, (1), pp. 217–223
- [13] Noguchi, T., Togashi, S., Nakamoto, R.: 'Short-current pulse based adaptive maximum-powerpoint tracking for photovoltaic power generation system'. Proc. Int. Symp. Industrial Electronics, 2000, vol. **1**, pp. 157–162
- [14] Liu, F., Duan, S., Liu, F., et al.: 'A variable step size INC MPPT method for PV systems', *IEEE Trans. Ind. Electron.*, 2008, **55**, (7), pp. 2622–2628
- [15] Abdouraziq, M.A., Maaroufi, M., Ouassaid, M.: 'A new variable step size INC MPPT method for PV systems'. Proc. Int. Conf. Multimedia Computing and Systems, 2014, pp. 1563–1568
- [16] Wu, W., Pongratananukul, N., Qiu, W., et al.: 'DSP-based multiple peak power tracking for expandable power system'. Proc. 18th Annual Conf. Exposition Applied Power Electronics, 2003, pp. 525–530
- [17] Xiao, W., Dunford, W.G.: 'A modified adaptive hill climbing MPPT method for photovoltaic power systems'. Proc. 35th Annual Conf. Power Electronics Specialists, 2004, vol. **3**, pp. 1957–1963
- [18] Haque, A.: 'Maximum power point tracking (MPPT) scheme for solar photovoltaic system', *Energy Technol. Policy*, 2014, **1**, (1), pp. 115–122
- [19] Femia, N., Petrone, G., Spagnuolo, G., et al.: 'Optimizing duty-cycle perturbation of P&O MPPT technique'. Proc. 35th Annual Conf. Power Electronics Specialists, 2004, vol. **3**, pp. 1939–1944
- [20] Masoum, M.A., Dehbonei, H., Fuchs, E.F.: 'Theoretical and experimental analyses of photovoltaic systems with voltage and current-based maximum power-point tracking', *IEEE Trans. Energy Convers.*, 2002, **17**, (4), pp. 514–522
- [21] Masoum, M., Dehbonei, H.: 'Design, construction and testing of a voltage-based maximum power point tracker (VMPTT) for small satellite power supply'. Proc. AIAA/USU Conf. on Small Satellites, 1999, Technical Session XII: Advanced Subsystem or Component Developments II. Available at <http://digitalcommons.usu.edu/smallsat/1999/all1999/88/>
- [22] Leedy, A.W., Guo, L., Aganah, K.A.: 'A constant voltage MPPT method for a solar powered boost converter with dc motor load'. Proc. Southeastcon, 2012, pp. 1–6
- [23] Aganah, K.A., Leedy, A.W.: 'A constant voltage maximum power point tracking method for solar powered systems'. Proc. 43rd Southeastern Symp. System Theory, 2011, pp. 125–130
- [24] Pandey, A., Dasgupta, N., Mukerjee, A.K.: 'A simple single-sensor MPPT solution', *IEEE Trans. Power Electron.*, 2007, **22**, (2), pp. 698–700
- [25] Elgendi, M.A., Zahawi, B., Atkinson, D.J.: 'Comparison of directly connected and constant voltage controlled photovoltaic pumping systems', *IEEE Trans. Sustain. Energy*, 2010, **1**, (3), pp. 184–192
- [26] Hohm, D., Ropp, M.E.: 'Comparative study of maximum power point tracking algorithms', *Prog. Photovolt. Res. Appl.*, 2003, **11**, (1), pp. 47–62
- [27] De Carvalho, P., Pontes, R., Oliveira, D., et al.: 'Control method of a photovoltaic powered reverse osmosis plant without batteries based on maximum power point tracking'. Proc. Conf. Exposition Transmission and Distribution, Latin America, 2004, pp. 137–142
- [28] Zhihao, Y., Xiaob, W.: 'Compensation loop design of a photovoltaic system based on constant voltage MPPT'. Proc. Conf. Power and Energy Engineering, Asia Pacific, 2009, pp. 1–4
- [29] Ma, J., Man, K.L., Ting, T., et al.: 'Dem: direct estimation method for photovoltaic maximum power point tracking', *Procedia Comput. Sci.*, 2013, **17**, pp. 537–544
- [30] Chatterjee, A., Keyhani, A., Kapoor, D.: 'Identification of photovoltaic source models', *IEEE Trans. Energy Convers.*, 2011, **26**, (3), pp. 883–889
- [31] Veerachary, M., Senju, T., Uezato, K.: 'Feedforward maximum power point tracking of PV systems using fuzzy controller', *IEEE Trans. Aerosp. Electron. Syst.*, 2002, **38**, (3), pp. 969–981
- [32] Andrejasic, T., Jankovec, M., Topic, M.: 'Comparison of direct maximum power point tracking algorithms using en 50530 dynamic test procedure', *IET Renew. Power Gener.*, 2011, **5**, (4), pp. 281–286
- [33] Xue, D., Chen, Y., Atherton, D.P.: 'Linear feedback control: analysis and design with MATLAB', 'Advanced in design and control' (Siam, Philadelphia, USA, 2007)
- [34] Mahmoud, Y.A., Xiao, W., Zeineldin, H.H.: 'A parameterization approach for enhancing PV model accuracy', *IEEE Trans. Ind. Electron.*, 2013, **60**, (12), pp. 5708–5716
- [35] Campbell, R.C.: 'A circuit-based photovoltaic array model for power system studies'. Proc. 39th North American Power Symp., 2007, pp. 97–101
- [36] Villalva, M.G., Gazoli, J.R., Ruppert, F.E.: 'Comprehensive approach to modeling and simulation of photovoltaic arrays', *IEEE Trans. Power Electron.*, 2009, **24**, (5), pp. 1198–1208

- [37] Kadri, R., Gaubert, J.P., Champenois, G.: ‘An improved maximum power point tracking for photovoltaic grid-connected inverter based on voltage-oriented control’, *IEEE Trans. Ind. Electron.*, 2011, **58**, (1), pp. 66–75
- [38] Sera, D., Teodorescu, R., Rodriguez, P.: ‘PV panel model based on datasheet values’. Proc. Int. Symp. Industrial Electronics, 2007, pp. 2392–2396
- [39] Rauschenbach, H.: ‘*Solar cells array design handbook: the principles and technology of photovoltaic energy conversion*’ (Van Nostrand Reinhold, New York, USA, 1980, 1st edn.)
- [40] Edri, E., Kirmayer, S., Cahen, D., et al.: ‘High open-circuit voltage solar cells based on organic–inorganic lead bromide perovskite’, *J. Phys. Chem. Lett.*, 2013, **4**, (6), pp. 897–902
- [41] Black, N., Moore, S.: Gauss–Seidel Method - From MathWorld - A Wolfram Web Resource: created by Weisstein, Eric W’. Available at <http://www.mathworld.wolfram.com/Gauss-SeidelMethod.html>, 2002
- [42] Ramanarayanan, V.: ‘Course material on switched mode power conversion’ (Indian Institute of Science, 2005, 2nd edn., 2006)
- [43] Bacha, S., Munteanu, I., Bratu, A.I.: ‘Power electronic converters modeling and control’, in Grimble, M.J., Johnson, M.A. (Eds): ‘*Advanced textbooks in control and signal processing*’ (Springer, London, UK, 2014)
- [44] Modabbernia, M.R., Sahab, A.R., Mirzaee, M.T., et al.: ‘The state space average model of boost switching regulator including all of the system uncertainties’, *Adv. Mater. Res., Trans Tech Publication Ltd.*, 2011, **403**, pp. 3476–3483
- [45] Sanders, S.R., Noworolski, J.M., Liu, X.Z., et al.: ‘Generalized averaging method for power conversion circuits’, *IEEE Trans. Power Electron.*, 1991, **6**, (2), pp. 251–259
- [46] Hauke, B.: ‘*Basic calculation of a boost converter’s power stage*’ (Dallas, Texas Instruments, 2009), pp. 1–9
- [47] Liu, S.I., Liu, J., Zhang, J.: ‘Research on output voltage ripple of boost DC/DC converters’. Proc. Int. Multi Conf. of Engineers and Computer Scientists, Citeseer, Hong Kong, March 2008, vol. 2, pp. 19–21
- [48] Arrigo, J.: ‘*Input and output capacitor selection*’. Texas Instruments, SLTA055, 2006
- [49] Enrique, J.M., Andújar, J.M., Bohórquez, M.A.: ‘A reliable, fast and low cost maximum power point tracker for photovoltaic applications’, *Sol. Energy*, 2010, **84**, (1), pp. 79–89

## 9 Appendix

### 9.1 Appendix 1

The trial and error approach for determining the gains  $K_p$  and  $K_i$  of the controller is an iterative procedure of successive changing of  $K_p$  and  $K_i$  until the response of the PV system becomes satisfactory, i.e. zero SSE with low overshoot and short settling

time. At first, set the controller to the P-mode only (i.e.  $K_i = 0$ ) and start with small value of  $K_p$ , say 0.5. Run the PV system with operating conditions at STC. For high overshoot, long settling time and large SSE, increase  $K_p$  with steps equal 0.5 and observe the rate of reduction of SSE. When the rate of SSE reduction starts to decrease, terminate the increase of  $K_p$  and start to use  $K_i$ . Start with small value of  $K_i$ , say 0.5, increase it in growing steps (say, by doubling the preceding step) and check the value of SSE. When the SSE value approaches zero, terminate the increase of  $K_i$  and switch to use  $K_p$  by increasing its value to decrease the resulting settling time. The procedure of switching between the increase of  $K_p$  and that of  $K_i$  continues until a satisfactory response of the PV system is achieved.

### 9.2 Appendix 2

The influence of temperature  $T$  (K) and radiation  $G$  (W/m<sup>2</sup>) on the PV module’s parameters is expressed as [30, 38]

$$I_{ph} = I_{ph\_ref} \times G/1000 \quad (9)$$

$$I_{sc} = I_{sc\_ref} \times G/1000 \quad (10)$$

$$I_{sc} = I_{sc} \times (1 + K_i/100 \times (T - 298)) \quad (11)$$

$$V_{oc} = n_s \times V_t \times \ln \left\{ \frac{I_{ph} \times R_{sh} - V_{oc}}{I_{o\_ref} \times R_{sh}} \right\} \quad (12)$$

$$V_{oc} = V_{oc} + K_v \times (T - 298) \quad (13)$$

$$I_o = I_{sc} \times \left\{ \frac{V_{oc} - I_{sc} \times R_s}{R_{sh}} \right\} \times \exp \frac{-V_{oc}}{n_s \times V_t} \quad (14)$$

$$I_{ph} = I_o \times \exp \frac{V_{oc}}{n_s \times V_t} + \frac{V_{oc}}{R_{sh}} \quad (15)$$